HIGH FIELD PULSE DIPOLE AND QUADRUPOLE MAGNETS FOR COMPACT MEDICAL PULSE SYNCHROTRON

K. Endo, K. Egawa and Z. Fang, KEK, Tsukuba, Japan
M. Mizobata, J. Matsui, K. Sako and Y. Kijima, Mitsubishi Electric Corp., Kobe, Japan
A. Nishikawa, F. Ohtani, S. Tokura and A. Yamamoto, IHI Co. Ltd., Yokohama, Japan

Abstract

Pulse dipole and quadrupole magnets are being developed for the compact proton synchrotron dedicated to the medical radiotherapy. The highest proton energy is 200MeV, which will cover more than 80% of patients, and the machine itself will be made compact and planned to promote the advanced cancer treatment by using accelerators. For this purpose the compact dipole magnet generating 3T at the peak current of 200kA was manufactured and tested by feeding the pulse excitation current of a half sinusoidal waveform having the rise and fall time almost equivalent to 50Hz. Quadrupole is also designed and will be manufactured in this fiscal year after an elaborate dynamical 3D computational design study. Detailed design works will be presented for both magnets and the beam dynamical issues based on the accelerator performance will be discussed in relation to the field properties.

INTRODUCTION

A compact 200 MeV proton synchrotron is being considered as one of candidates to promote the advanced cancer treatment based on the accelerator. The maximum proton energy is less compared to the existing medical synchrotron. In most cases about 80% of patients were treated with the proton energy less than 200 MeV from the statistical depth distribution of the diseased parts [1]. The proton and carbon-ion are recognized more effective than the photon and electron as the formers have a distinct range beyond which no radiation dose reaches. At the end of the range there is so-called Bragg peak where the rest of the kinetic energy is released in a very short distance giving the fatal dose to the surrounding tissue.

The proton synchrotron is less expensive and smaller than that of heavy ion for the same penetration depth of the accelerated particles. It is desirable to develop the cost effective medical accelerator which is reliable and can be installed at reasonable cost even at local hospitals. These should have complementary roles to the regional medical centers which equip with more powerful medical accelerator of proton and/or heavy ion. The latter mainly serves to patients whose treatment protocols exceed the performance of the former, in addition to the therapeutic researches. In this sense the present works are devoted to the development of the medical accelerator for hospitals and the reason why the synchrotron is chosen is that the pulse synchrotron can easily change the beam energy.

LATTICE AND MAGNETS

Lattice

The original lattice design composed of the quadrupole triplet benefits from the fine tuning for both horizontal and vertical betatron oscillations independently [2]. It is modified to use only defocusing quadrupoles with the magnet configuration of DOB. To make the synchrotron ring as small as possible it is inevitable to adopt the high field dipole magnet exceeding the saturation limit. The maximum excitation of 3 T at 200 MeV is considered modest and every effort in the past was focused on the development of the 3 T dipole magnet of which full size model was manufactured as shown in Fig.1 [3, 4]. Fortunately it has an expected performance given by the 3D dynamic field simulations [5].

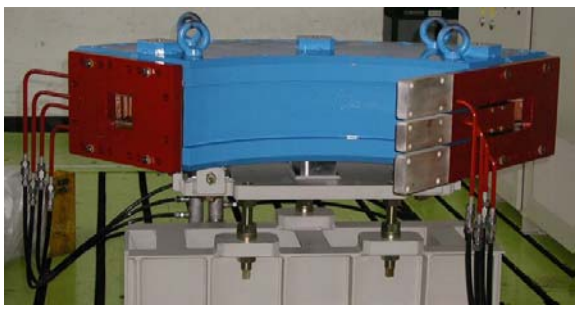

Figure 1: Dipole magnet.

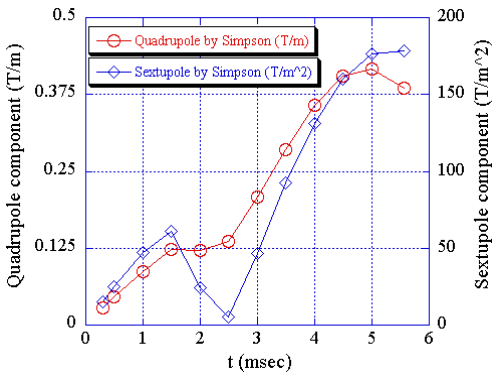

Figure 2: Quadrupole and sextupole components in the dipole magnet obtained by the field measurement.

The measured quadrupole and sextupole field components of the dipole magnet are shown in Fig.2. The sextupole component is corrected by the independent sextupoles in addition to the correction coils in each dipole. The effect by the quadrupole component must be compensated by using the main quadrupole magnets.

Considering the quadrupole field component in the beam optics simulation as a thin lens approximation, its contribution is a focusing element in the dipole magnet. To distribute the quadrupole component uniformly, the dipole is sliced into 21 elements between which 20 thin lens quadrupoles are inserted. The tune variation due to the quadrupole error field is shown in Fig.3 and Fig.4 compares the beam parameters both with and without the quadrupole error field.

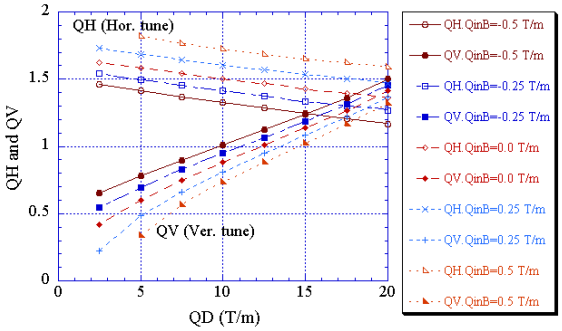

Figure 3: Tune variations due to the quadrupole error field (-0.5 ~ 0.5 T/m) in the dipole magnet as a function of the 15cm QD strength at 200 MeV.

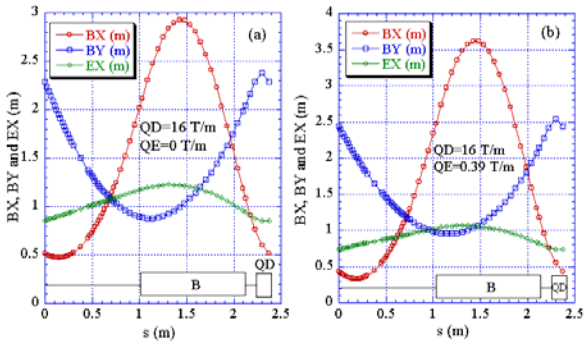

Figure 4: Beam parameters for (a) no quadrupole error field (QE=0 T/m) and (b) QE=0.39 T/m at 200MeV.

For the positive quadrupole error field the dispersion function decreases, but the field error more than 0.75 T/m is not allowed in the lattice shown in Fig.4. As the present dipole magnet gives small positive quadrupole component, the lattice parameters suffer small changes. The particle behaviour observed at the long straight section in the presence of only quadrupole field in the dipole is given for the injection field in Fig.5.

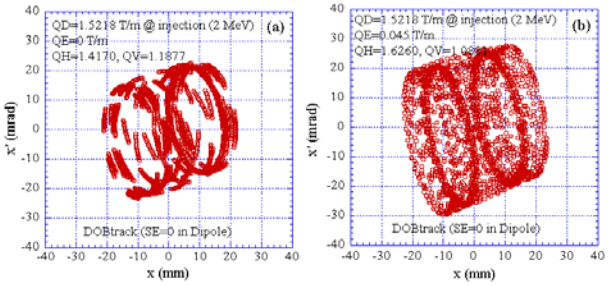

Figure 5: Particle tracking at injection for (a) no quadrupole error field (QE=0) and (b) QE=0.045 T/m.

In Fig.5 the particle momentum varies from -1% to +1% by the RF acceleration and the quadrupole error field alters the twiss parameters.

There exists a large sextupole error field in the dipole (Fig.2) which is not corrected merely by the independent sextupole magnets. By applying the correction windings to the dipole it should be reduced less than 2.5 T/m^2 for which the particle tracking is given in Fig.6.

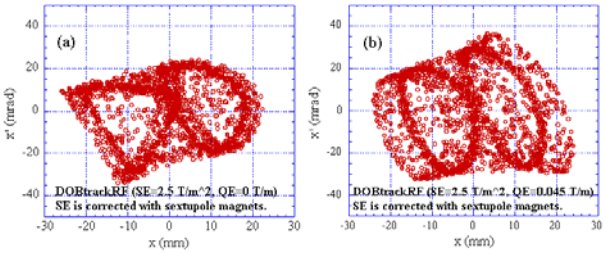

Figure 6: Particle tracking at injection for (a) sextupole error field (SE=2.5 T/m^2) and QE=0, and (b) SE=2.5 T/m^2 and QE=0.045 T/m. Sextupole error field is corrected in both cases.

Dipole Magnet

A big modification in the dipole magnet design is to replace the present coil made from the strand cable with the hollow conductor made of OFC (Oxygen Free Copper). The heat conductivity of the strand cable is inferior to the hollow conductor because of lacking the metallic contact between strands. To increase the repetition rate a good heat conduction is desirable. However, the eddy current in the hollow conductor has an effect to the field distribution in the magnet gap.

By the time-dependent 3D simulation which treats the eddy current, two cases with and without eddy current are compared. Fig.7 shows both cases at 3 msec during the acceleration time of 5 msec. 'No-eddy' means the case of strand cable and 'Eddy-01' and 'Eddy-02' are for the hollow conductor. Difference of Eddy-02 from Eddy-01 is only the conductor cut at the corner where the current density is large but its effect is almost nothing.

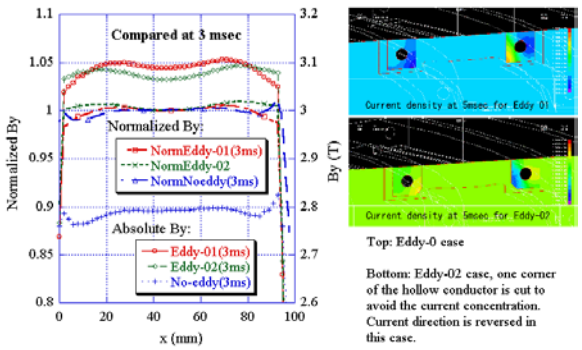

Figure 7: Field distributions of the dipole magnet at 3 msec by the time-dependent 3D simulation. Cases of Eddy-01 and Eddy-02 differ only in the conductor cross-section as shown in the right.

It seems no essential difference in the field distribution between the strand cable and hollow conductor except

that the absolute flux density in the gap is higher to the hollow conductor than the strand cable. It is explained that the eddy current in the hollow conductor confines the flux inside the gap as shown in Fig.8 where the By distributions for 3 cases in Fig.7 are given by a color code at the maximum field, 3T.

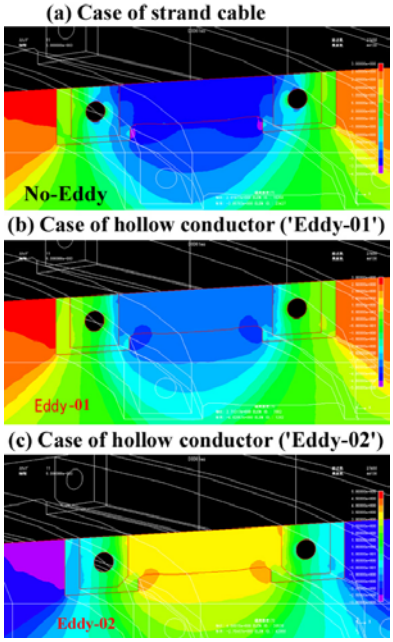

Figure 8: Flux density (By) distributions for 3 cases shown in Fig.7 are given by the color code.

Quadrupole Magnet

As shown in Fig.3 the operating point can be chosen to avoid the dangerous tunes by considering the effect of the gradient error in the dipole. The maximum field gradient is 30 T/m with the effective length of 15 cm (Fig.9). If QF's are required in the future, the present circumference of 9.5 m is resumed by the original 11.9 m to accommodate them (8 QF's) with applying modifications to the bus-bar systems of dipole and quadrupole magnets.

The computational gradient distributions for several pole-shim arrangements and the effective gradient length are given in Fig.10 for the chamfered pole ends of 10 mm by 20 mm in length and height (Fig.11), respectively.

Coil is made from the hollow conductor in 5 turns/pole and fits in the narrow spaces close to the horizontal and vertical axes allowing larger useful aperture as shown in Fig.10(a).

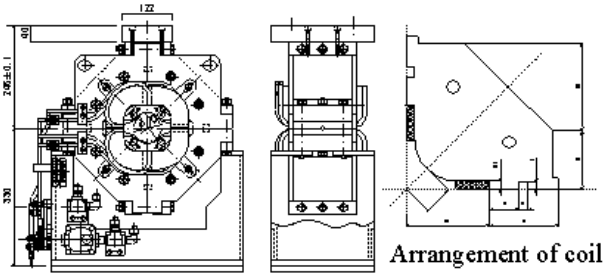

Figure 9: Quadrupole magnet.

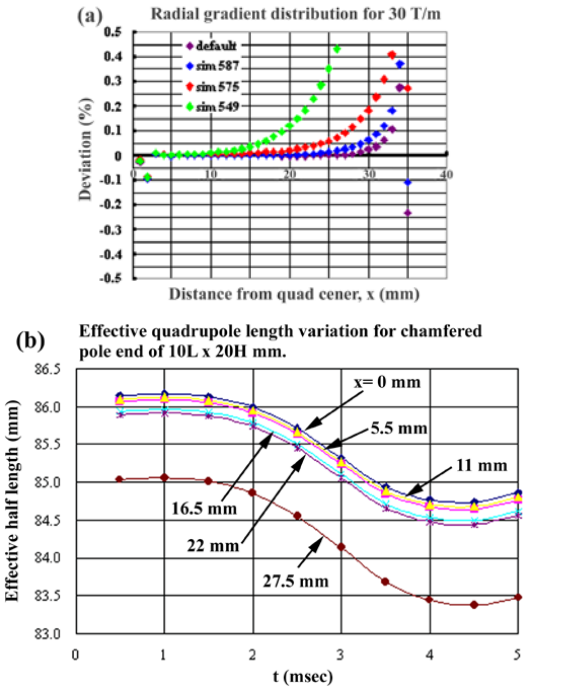

Figure 10: Computational gradient distributions (a) for several shim arrangements and the effective gradient length (b) for the chamfered pole ends of 10 x 20 mm (length x height).

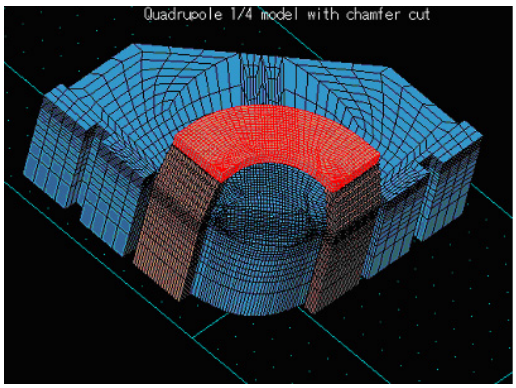

Figure 11: Chamfered pole end.

REFERENCES

[1] Y. Hirao, "Results from HIMAC and Other Therapy Facilities in Japan," Proc. Cyclotrons 2001, pp.8-12.

[2] K. Endo et al., "Compact Proton and Carbon Ion Synchrotrons for Radiation Therapy," Proc. EPAC2002, Paris, pp.2733-5.

[3] K. Endo et al., "Development of Compact Proton Synchrotron for Radiation Therapy," Proc. ARTA2003, Tokyo, pp.51-4.

[4] K. Endo et al., "Development of High Field Dipole and High Current Pulse Power Supply for Compact Proton Synchrotron," Proc. PAC2003, Portland, pp.1071-3.

[5] K. Endo et al., "Development of High Field Dipole Magnet and Power Supply for Proton Therapy," Proc. 14th SAST, Tsukuba, 2003, pp.196-8.